

# A SIMPLIFIED APPROACH TO STAGGERED PRT CLUTTER FILTERING

GREGORY MEYMARIS\*

*National Center for Atmospheric Research, Boulder, Colorado*

JOHN C. HUBBERT

*National Center for Atmospheric Research, Boulder, Colorado*

GRANT GRAY

*Advanced Radar Corporation, Boulder, Colorado*

## 1. Introduction

Staggered PRT (pulse repetition) is a popular technique to mitigate the range-velocity dilemma of weather radars. The unambiguous range is based on the longer PRT while the difference of the two PRTS (when the stagger is  $m/(m+1)$  for some positive integer  $m$ ) gives the unambiguous velocity (Zrnić and Mahapatra 1985). The major limitation of the staggered PRT technique has been clutter filtering. Since the time-series for a resolution volume is not equi-spaced, traditional filtering techniques such as time domain IIR (infinite impulse response) filtering or spectral domain filtering (based on the Discrete Fourier Transform (DFT)) are not applicable. Recently Sachidananda and Zrnić (2000; 2002) introduced a staggered PRT clutter filtering algorithm based on the interpolation of the time-series to equi-spaced samples. This is done by interleaving zeros into the time-series to create equi-spaced time-series. The interpolated time-series is then transformed with a DFT. The resulting spectrum contains 5 replicas of the intrinsic underlying spectrum. Fairly complicated matrix mathematics is used to filter the spectra and estimate the power, mean velocity, and spectrum width.

In this paper we introduce a novel technique in which the time-series is separated into two equi-spaced time-series and then a spectral notch clutter filter can be employed. The two filtered sequences are then recombined to once again create a staggered PRT sequence. The velocity and power can then be calculated in standard fashion.

## 2. A Simplified Staggered PRT Clutter Filter

A typical staggered PRT sequence is shown in Fig. 1. Sequence (A) is the staggered PRT sequence with the two staggers periods  $T_1$  and  $T_2$ ; in this paper, the  $2/3$  stagger is assumed, which means that  $T_1 = 2T_2/3$ . Denote the time-series samples  $s_1, s_2, \dots, s_M$  (where  $M$  is the total number of samples). Two sequences are created by taking alternate samples and separating them as indicated by the red and blue lines and the even and odd samples. The resulting two sequences have a period of  $T_1 + T_2$ . These equi-spaced sequences can then be filtered in the time domain or the frequency domain. If they are filtered in the frequency domain, the sequences are subsequently transformed using an inverse DFT. The resulting time-series are then interleaved to produce the filtered staggered PRT sequence corresponding to Fig. 1A.

It is instructive to compare the Sachidananda and Zrnić (2002) technique (SACHI) and the simplified staggered PRT technique (SSPRT) via a numerical example. Let  $T_1 = 1$  ms and  $T_2 = 1.5$  ms so that  $T_1 + T_2 = 2.5$  ms. The SACHI zero-interpolated sequence has a period  $T_u = 0.5$  ms. Therefore, the unambiguous velocity for SACHI is  $50 \text{ m s}^{-1}$  while the unambiguous velocity for SSPRT sequence, based on period of 2.5 ms, is  $10 \text{ m s}^{-1}$ . The SACHI technique creates 5 replicas of the true clutter signal spectrum equi-spaced over the entire unambiguous velocity range of  $50 + 50 = 100 \text{ m s}^{-1}$ . Thus the spectrum replicas are separated  $20 \text{ m s}^{-1}$  intervals. The performance of the SACHI clutter filter degrades when there is weather located at these  $20 \text{ m s}^{-1}$  intervals (i.e., weather can be eliminated by the clutter filter causing biased velocity and reflectivity estimates). For SSPRT, if weather signal

\* Corresponding author address:

Gregory Meymaris, RAL, NCAR  
1850 Table Mesa Dr., Boulder, CO 80305  
E-mail: meymaris at ucar.edu

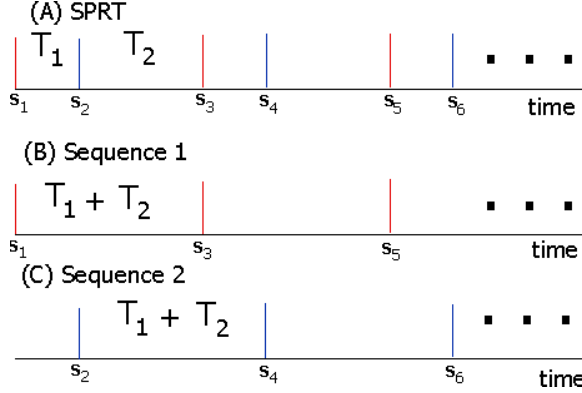


Figure 1: (A) A staggered PRT sequence. (B) and (C) show two equi-spaced sequences consisting of the even and odd samples of (A).

is located close to  $0 \text{ m s}^{-1}$ , this weather signal can also be attenuated causing biased estimates. Since the unambiguous velocity is  $10 \text{ m s}^{-1}$ , weather with  $20k \text{ m s}^{-1}$ , where  $k$  is an integer, will “wrap back” to  $0 \text{ m s}^{-1}$  and thus these weather signals can also be attenuated by the clutter filter. Therefore, both SACHI and SSPRT can suffer performance degradation when weather has velocity close to  $20k \text{ m s}^{-1}$  (depending on the width of the clutter filter). We next compare the performance of SACHI and SSPRT.

### 3. Simulations

To evaluate and compare different clutter filters, random complex time-series data were generated for various operational settings (number of pulses per time-series ( $M$ ) and pulse repetition frequency (PRT), and clutter filter settings (notch width), as well as various weather/clutter conditions (true weather mean velocity, spectrum width, signal-to-noise ratio (SNR), clutter-to-signal ratios (CSR)). An I&Q simulation technique was used based on the method described in Frehlich and Yadlowsky (1994); Frehlich (2000); Frehlich et al. (2001) except that the autocorrelation function is that of a weather echo as defined as in Doviak and Zrnić (1993, p. 125). This is a preferable method for generating complex time-series with a given average autocorrelation function, as opposed to what is described by Zrnić (1975), because it is not necessary to generate as long of a time-series in order to get the correct temporal statistics. In order to simulate staggered PRT sequences, the I&Q simulator is used to generate evenly spaced data at the higher “common” PRT ( $T_2 - T_1$ ), and then down-sample.

The simulation parameter settings in this paper

are as follows: 1000 time-series for each scenario, wavelength ( $\lambda$ ) of 10 cm, noise power of  $-80 \text{ dB}$ , clutter spectrum width  $0.28 \text{ m s}^{-1}$ , PRT of  $785 \mu\text{s}$  and  $1000 \mu\text{s}$ ,  $M$  of 32 and 64, mean velocities ranging across the Nyquist interval, spectrum width (weather) of 2 and  $4 \text{ m s}^{-1}$ , SNR of 10 dB and 20 dB, and CSR of  $-40 \text{ dB}$  to 50 dB.

Each time-series is processed using 2 different methods: the SACHI method and the SSPRT method. The SSPRT method works as follows. The time-series is separated into even and odd time-series (each with PRT  $T_1 + T_2$ ). The time-series are windowed using von Hann window function, and the FFT is computed. The two spectra are then each filtered using the Gaussian Model Adaptive Processing (GMAP) clutter filter (Siggia and R. Passarelli 2004). If GMAP determines that clutter exists, then GMAP not only attempts to remove the clutter power, it also attempts to reconstruct the weather by assuming a Gaussian shape. Normally, this is useful, but for staggered PRT data it would be necessary to also reconstruct the phases as well. For this analysis, the spectral bins identified by GMAP as containing clutter were simply set to zero, i.e. GMAP is used to identify the width for a notch filter. An inverse FFT is then applied to each spectrum, and the time-series are “zippered” back together. The power, mean velocity and spectrum width can then be calculated using the standard techniques (Zrnić and Mahapatra 1985; Sachidananda et al. 1999; Torres et al. 2004).

### 4. Model Results

First we compare the clutter suppression capabilities of SACHI and SSPRT (labelled SSCF) for a few cases. In these figures the left panel shows the bias of the output power (compared to the true weather power) and the right panel is the standard deviation of the estimate in dB; the x-axis in both plots is CSR. In figure 2 the SNR is 10 dB, PRT is  $785 \mu\text{s}$ ,  $M$  is 64, and the weather mean velocity is  $13 \text{ m s}^{-1}$ , in figure 3, the SNR is 10 dB, PRT is  $1000 \mu\text{s}$ ,  $M$  is 64, and the weather mean velocity is  $10 \text{ m s}^{-1}$ , and in figure 4 the SNR is 10 dB, PRT is  $785 \mu\text{s}$ ,  $M$  is 64, and the weather mean velocity is  $13 \text{ m s}^{-1}$ . These plots show that for these cases that the SSPRT technique performs comparably to SACHI. For 64 points SSPRT, in fact, performs better (less bias and lower standard deviations), although the technique performs worse in the 32 point case.

Finally we compare the power and velocity re-

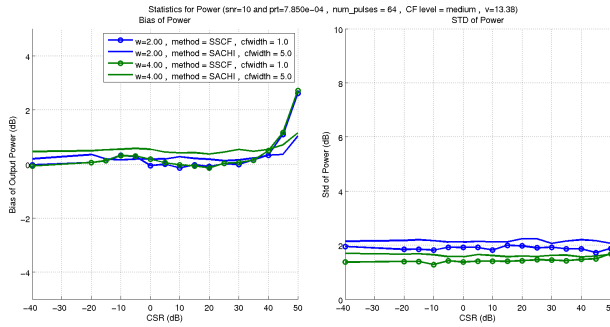


Figure 2: A performance comparison of SACHI and SSPRT (labelled SSCF). The left panel shows the bias of the output power (compared to the true weather power) as a function of CSR. The SNR is 10 dB, PRT is 785  $\mu$ s,  $M$  is 64, and the weather mean velocity is 13  $\text{m s}^{-1}$ . The right panel is the same except that the standard deviation of the estimate in dB is shown.

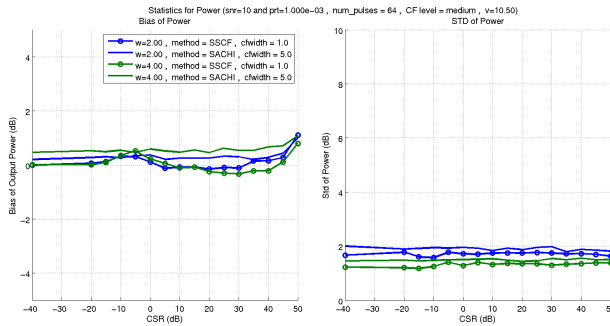


Figure 3: A performance comparison of SACHI and SSPRT (labelled SSCF). The left panel shows the bias of the output power (compared to the true weather power) as a function of CSR. The SNR is 10 dB, PRT is 1000  $\mu$ s,  $M$  is 64, and the weather mean velocity is 10  $\text{m s}^{-1}$ . The right panel is the same except that the standard deviation of the estimate in dB is shown.

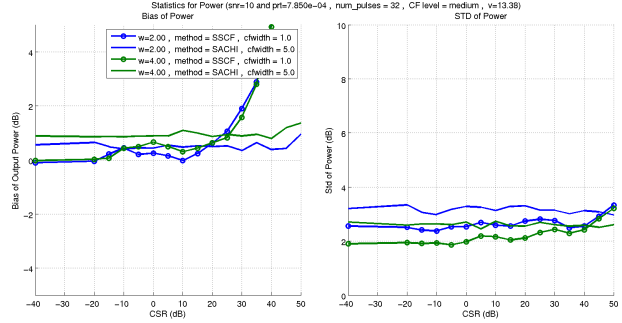


Figure 4: A performance comparison of SACHI and SSPRT (labelled SSCF). The left panel shows the bias of the output power (compared to the true weather power) as a function of CSR. The SNR is 10 dB, PRT is 785  $\mu$ s,  $M$  is 32, and the weather mean velocity is 13  $\text{m s}^{-1}$ . The right panel is the same except that the standard deviation of the estimate in dB is shown.

covery capabilities of SACHI and SSPRT (labelled SSCF), for one case, as a function of the input weather velocity. In figure 5, the top left panel shows the bias of the output power (compared to the true weather power), the top right panel is the standard deviation of the estimate in dB, the bottom left is the (circular) mean bias of recovered velocity, and the bottom right is the standard deviation. In this figure, the SNR is 10 dB, PRT is 785  $\mu$ s,  $M$  is 64, and the weather mean velocity is 13  $\text{m s}^{-1}$ . This plot shows that for these cases that the SSPRT technique performs comparably to SACHI, except at the “fifths” where the current version of SSPRT is performing worse.

## 5. Conclusions

The SSPRT technique is a promising clutter filtering technique in at least some scenarios. It has the advantage that it is quite simple, building from more standard techniques than does SACHI. There are still various refinements that could be made to the method. For example notch filters induce biases in power, velocity and spectrum width, and so trying to use GMAP’s reconstruction may be very advantageous. For example, the power could be recovered based on the GMAP reconstruction or perhaps the spectral phase information could be reconstructed (GMAP only reconstructs the power). Furthermore, a detailed study of the scenarios in which SSPRT is better than SACHI, and vice versa, needs to be performed.

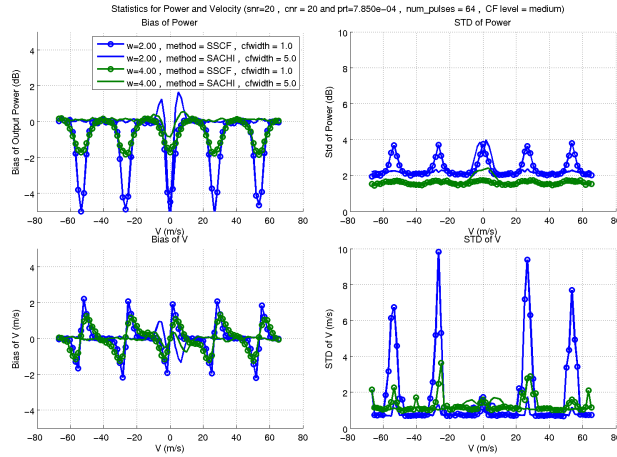


Figure 5: A performance comparison of SACHI and SSPRT (labelled SSCF). In this figure the top left panel shows the bias of the output power (compared to the true weather power), the top right panel is the standard deviation of the estimate in dB, the bottom left is the (circular) mean bias of recovered velocity, and the bottom right is the standard deviation. A performance comparison of SACHI and SSPRT (labelled SSCF). The SNR is 20 dB, CSR is 0 dB, PRT is 785  $\mu$ s,  $M$  is 64.

## 6. Acknowledgment

This research was supported in part by the ROC (Radar Operations Center) of Norman OK. The National Center for Atmospheric Research is sponsored by the National Science Foundation. Any opinions, findings and conclusions or recommendations expressed in this publication are those of the author(s) and do not necessarily reflect the views of the National Science Foundation.

## References

- Doviak, R. J. and D. S. Zrnić: 1993, *Doppler Radar and Weather Observations*, Academic Press, San Diego, California. 2nd edition.
- Frehlich, R., 2000: Simulation of coherent doppler lidar performance for space-based platforms. *Journal of Applied Meteorology*, **39**, 245–262.
- Frehlich, R., L. B. Cornman, and R. Sharman, 2001: Simulation of three-dimensional turbulent velocity fields. *Journal of Applied Meteorology*, **40**, 246–258.
- Frehlich, R. and M. J. Yadlowsky, 1994: Performance of mean-frequency estimators for doppler

radar and lidar. *Journal of Atmospheric and Oceanic Technology*, **11**, 1217–1230, corrigenda, **12**, 445–446.

- Sachidananda, M. and D. Zrnić, 2000: Clutter Filtering and Spectral Moment Estimation for Doppler Weather Radars Using Staggered Pulse Repetition Time (PRT). *Journal of Atmospheric and Oceanic Technology*, **17**, 323–331.
- Sachidananda, M. and D. Zrnic, 2002: An Improved Clutter Filtering and Spectral Moment Estimation Algorithm for Staggered PRT Sequences. *Journal of Atmospheric and Oceanic Technology*, **19**, 2009–2019.

Sachidananda, M., D. S. Zrnić, and R. J. Doviak, 1999: Signal design and processing techniques for WSR-88D ambiguity resolution. part-3. Technical report, National Severe Storms Laboratory.

Siggia, A. and J. R. Passarelli: 2004, Gaussian model adaptive processing (gmap) for improved ground clutter cancellation and moment calculation. *Proceedings of Third European Conference on Radar in Meteorology and Hydrology*, ERAD, Visby, Gotland, Sweden, 67–73.

Torres, S., M. Sachidananda, and D. S. Zrnić, 2004: Signal design and processing techniques for WSR-88D ambiguity resolution: Phase coding and staggered PRT data collection, implementation, and clutter filtering. part-8. Technical report, National Severe Storms Laboratory.

Zrnić, D. S., 1975: Simulation of weatherlike doppler spectra and signals. *Journal of Applied Meteorology*, **14**, 619–620.

Zrnić, D. S. and P. Mahapatra, 1985: Two Methods of Ambiguity Resolution in Pulse Doppler Weather Radars. *Aerospace and Electronic Systems, IEEE Transactions on*, **AES-21**, 470–483.